

ARTICLE

Ultrasonic Study on Charge Ordering in $\text{Nd}_{0.5}\text{Ca}_{0.5}\text{Mn}_{1-x}\text{Al}_x\text{O}_3$ ($x=0,0.03$)

Yi Liu, Hui Kong, Jin-rui Su, Chang-fei Zhu*

Laboratory of Advanced Functional Materials and Devices, Department of Materials Science and Engineering, University of Science and Technology of China, Hefei 230026, China

(Dated: Received on March 20, 2006; Accepted on April 18, 2006)

The ultrasonic, magnetic and transport properties of $\text{Nd}_{0.5}\text{Ca}_{0.5}\text{Mn}_{1-x}\text{Al}_x\text{O}_3$ ($x=0, 0.03$) were studied from 15 to 300 K. The temperature dependencies of resistivity and magnetization show that $\text{Nd}_{0.5}\text{Ca}_{0.5}\text{MnO}_3$ undergoes a charge ordering transition at $T_{\text{CO}}\sim 257$ K. An obvious softening of the longitudinal sound velocity above T_{CO} and a dramatic stiffening below T_{CO} accompanied by an attenuation peak were observed. These features imply a strong electron-phonon interaction via the Jahn-Teller effect in the sample. Another broad attenuation peak was observed at around $T_p\sim 80$ K. This anomaly is attributed to the phase separation between the antiferromagnetic (AFM) and paramagnetic (PM) phases and gives a direct evidence for spin-phonon coupling in the compound. For the $x=0.03$ sample, both the minimum of sound velocity and attenuation peaks shift to a lower temperature. The results indicate that the charge ordering and CE-type AFM state in $\text{Nd}_{0.5}\text{Ca}_{0.5}\text{MnO}_3$ are both partially suppressed by replacing Mn with Al.

Key words: Manganite, Charge ordering, Phase separation, Ultrasonic velocity and attenuation**I. INTRODUCTION**

In recent years, the hole-doped perovskite manganites $\text{Ln}_{1-x}\text{A}_x\text{MnO}_3$ (Ln=rare earth metal and A=alkaline earth metal) have received much attention due to their 'colossal magnetoresistance' effect (CMR) [1-4]. These compounds show a strong coupling among spin, charge and lattice degree of freedom [5-7]. Many related physical phenomena such as charge and orbital ordering [8-10], metal-insulator transition [11,12] and phase separation [13,14] have been studied. Recent studies for manganites [15,16] have revealed that the CMR effect is attributed not only to the double-exchange (DE) interaction but also to other interactions and competitions, such as charge-orbital ordering and electron-phonon coupling. The charge ordering (CO) state is often observed in half-doped perovskite-type manganites $\text{R}_{0.5}\text{A}_{0.5}\text{MnO}_3$, where the Mn^{3+} and Mn^{4+} are involved in an order arrangement with localized e_g electrons [8-10]. Recently, it has been found that the charge ordering transition does not necessarily lead to a simultaneous long-range ordering of magnetic moments. In $\text{Nd}_{0.5}\text{Ca}_{0.5}\text{MnO}_3$ [17-20], it was found that the charge ordering occurs at a much higher temperature than the CE-type antiferromagnetic (AFM) ordering ($T_{\text{CO}}\sim 250$ K, $T_{\text{N}}\sim 160$ K). In addition, from either resistivity or magnetization study alone, it is impossible to determine the co-existence of a charge ordering transition and an AFM transition. So it is necessary to further investigate the charge ordering state and related magnetic properties in $\text{Nd}_{0.5}\text{Ca}_{0.5}\text{MnO}_3$ where charge-ordering and AFM ordering occur at different temperatures.

The ultrasonic technique is a very sensitive tool for probing systems undergoing magnetic and structural phase transitions, and it has been proven to be successful in studying electron-phonon and spin-phonon coupling in hole-doped manganites [21-26]. In this article, we report on the ultrasonic, magnetic and transport properties of Al doping in the Mn site of half-doped $\text{Nd}_{0.5}\text{Ca}_{0.5}\text{MnO}_3$, concentrating on the temperature region around CO and AFM.

II. EXPERIMENTS

Polycrystalline samples of $\text{Nd}_{0.5}\text{Ca}_{0.5}\text{Mn}_{1-x}\text{Al}_x\text{O}_3$ ($x=0,0.03$) were prepared by the standard solid-state reaction processing. The well-mixed stoichiometric mixture of high-purity Nd_2O_3 , CaCO_3 , MnO_2 and Al_2O_3 were calcined at 1000 and 1100 °C for 15 h in air with intermediate grinding, respectively. After that, the as-obtained powder was pressed into pellets and sintered at 1320 °C for 15 h in air and then cooled to room temperature. The structure of the sample was determined by a powder X-ray diffractionmeter (Japan MXP18AHF, MAC Science Co. Ltd.) using $\text{Cu K}\alpha$ radiation ($\lambda=1.54056$ Å). It was found that all samples are of single phase with an orthorhombic structure (space group Pnma).

Magnetization measurements were performed in bulk samples using a superconducting quantum interference device (SQUID) magnetometer from Quantum Design (MPM-5). The electrical resistivity of the sample was measured as a function of temperature by the standard four-probe technique. The ultrasonic velocity and attenuation measurements were performed on the Matec-7700 series by a conventional pulsed-echo-overlap technique. Longitudinal ultrasonic wave pulses were generated by a 10 MHz X-cut quartz transducer. The relative

* Author to whom correspondence should be addressed. E-mail: cfzhu@ustc.edu.cn

change of sound velocity is defined as

$$\frac{\Delta V}{V} = \frac{V - V_{\min}}{V_{\min}} \quad (1)$$

where V_{\min} is the minimum sound velocity over entire temperature region studied. The ultrasonic attenuation was calculated from the exponential decay of the pulse echoes, and expressed as:

$$\alpha = -\frac{20}{2(m-n)L} \log \frac{V_m}{V_n} \quad (2)$$

where V_m and V_n are the maximum amplitude (voltage) of the m th and the n th pulse echoes, respectively.

III. RESULTS AND DISCUSSION

Figure 1 shows the resistivity of the $\text{Nd}_{0.5}\text{Ca}_{0.5}\text{MnO}_3$ and $\text{Nd}_{0.5}\text{Ca}_{0.5}\text{Mn}_{0.97}\text{Al}_{0.03}\text{O}_3$ as a function of temperature. It can be seen that both the samples exhibit semiconductor behavior over the entire temperature range, from 300 K down to 15 K. The resistivity shows a discernible change in the slope around the charge ordering transition temperature T_{CO} , implying the onset of the charge ordering transition. The resistivity data display a variable-range hopping (VRH) process below T_{CO} . The model of VRH can be expressed as [27]:

$$R = R_0 \exp\left(\frac{T_0}{T}\right)^{1/4} \quad (3)$$

where T_0 is the Mott's activation energy (in units of K) and can be expressed as

$$T_0 = \frac{21}{k_{\text{B}}N(E)\xi^3} \quad (4)$$

where k_{B} is Boltzmann's constant, $N(E)$ is the density of state, and ξ is the localization length. It was found that Al doping does not change the VRH behavior in the CO state region. However, an increase in the localization length ξ with Al-doping was observed, presuming that the density of state $N(E)$ does not change. The inset of Fig.1 shows the $\ln\rho(T)-T^{-1/4}$ curve of $\text{Nd}_{0.5}\text{Ca}_{0.5}\text{MnO}_3$ and $\text{Nd}_{0.5}\text{Ca}_{0.5}\text{Mn}_{0.97}\text{Al}_{0.03}\text{O}_3$. The activation energies of 3.366×10^8 and 1.831×10^8 K in the CO states are obtained respectively.

The temperature dependencies of magnetization of the samples are shown in Fig.2. A pronounced peak can be seen near T_{CO} for $\text{Nd}_{0.5}\text{Ca}_{0.5}\text{MnO}_3$, which indicates the charge ordering transition. Below 100 K, the magnetization begins to increase with decreasing temperature, which is usually ascribed to the PM behavior of Nd ions [17-20]. The results show that replacing Mn with Al partially suppresses the magnetization peak and shifts it to a lower temperature, clearly indicating the weakening of the CO state.

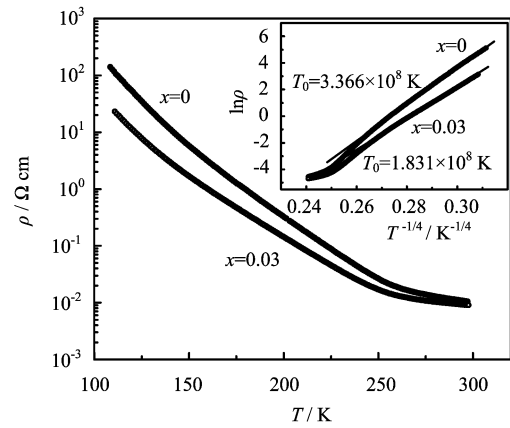


FIG. 1 Temperature dependence of the electrical resistivity for $\text{Nd}_{0.5}\text{Ca}_{0.5}\text{Mn}_{1-x}\text{Al}_x\text{O}_3$. Inset is the $\ln\rho$ versus $T^{-1/4}$ curves.

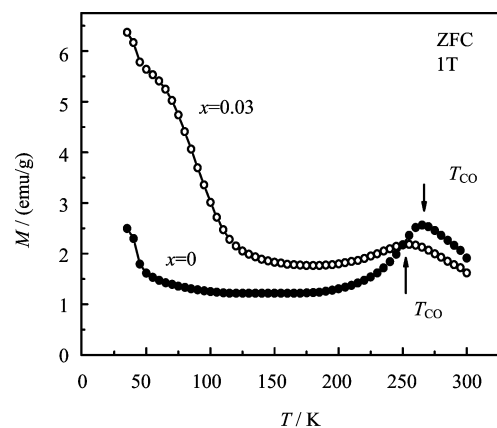


FIG. 2 Temperature dependence of the magnetization for $\text{Nd}_{0.5}\text{Ca}_{0.5}\text{Mn}_{1-x}\text{Al}_x\text{O}_3$.

Figure 3 shows ultrasonic velocity and attenuation versus temperature for the samples, measured by 10 MHz longitudinal waves from 300 and 15 K. For $\text{Nd}_{0.5}\text{Ca}_{0.5}\text{MnO}_3$, the longitudinal sound velocity shows a slight softening accompanied by a sharp attenuation peak as cooling down from room temperature to T_{CO} . Just below T_{CO} , the sound velocity stiffens dramatically. From earlier studies [21-26], it is suggested that this ultrasonic anomaly originates from the strong electron-phonon coupling via Jahn-Teller distortion of Mn^{3+} ions. The strength of the JT coupling in the CO state can be estimated from the measurement of the longitudinal modulus. The longitudinal modulus C_l is calculated using the following formula [28]:

$$C_l = DV_l^2 \quad (5)$$

where D is the mass density and V_l is the longitudinal ultrasonic velocity. According to the cooperative Jahn-Teller theory, one can obtain the relationship between the elastic modulus $C_l(T)$ and the temperature T above

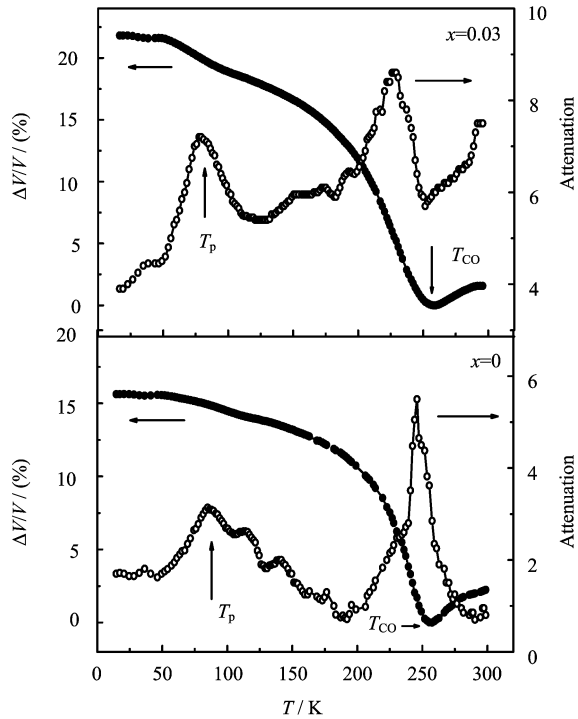


FIG. 3 Temperature dependence of the ultrasonic longitudinal sound velocity and attenuation for $\text{Nd}_{0.5}\text{Ca}_{0.5}\text{Mn}_{1-x}\text{Al}_x\text{O}_3$ ($x=0, 0.03$)

T_{CO} as follows [29]:

$$C_l(T) = C_0 \frac{T - T_c^0}{T - \Theta} \quad (6)$$

The characteristic temperature T_c^0 and Θ can be determined by the fitting of the elastic softening above T_{CO} . The Jahn-Teller coupling energy is given by $E_{JT} = T_c^0 - \Theta$ [30,31]. In Fig.4, the experimental data (open symbols) and fitting results (solid line) by Eq.(3) at the temperatures above T_{CO} are shown. The good fit of the theoretical results (the values of the T_c^0 , Θ , E_{JT} are 182, 170 and 12 K, respectively) to the data indicates that the Jahn-Teller effect is the dominant mechanism responsible for the CO state in the compound. On the other hand, from the ultrasonic measurements we can clearly see that the doping of nonmagnetic Al affects the charge ordering state dramatically. When Al replaces the magnetic ion Mn, the minimum of sound velocity (V_{min}) and the attenuation peak shift to lower temperature, indicating the partial suppression of the CO state.

Another interesting phenomenon in the experimental results is the attenuation anomaly at low temperature. For $\text{Nd}_{0.5}\text{Ca}_{0.5}\text{MnO}_3$, a broad attenuation peak accompanied by a slight softening in sound velocity is observed at $T_p \sim 80$ K. From the magnetic study of $\text{Nd}_{0.5}\text{Ca}_{0.5}\text{MnO}_3$, the steep increase of magnetization is observed just below T_p , which has been ascribed to the PM ordering of Nd ions. So the anomalous attenuation

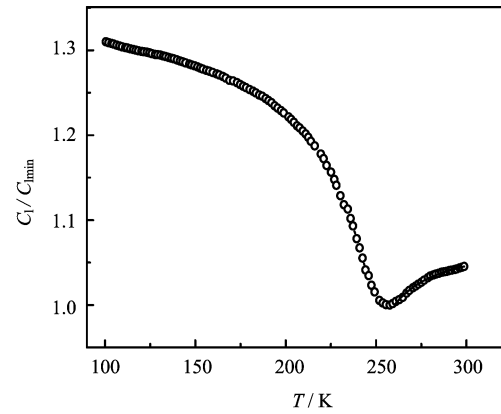


FIG. 4 The longitudinal modulus $C_l(T)$ as a function of temperature for $\text{Nd}_{0.5}\text{Ca}_{0.5}\text{MnO}_3$. Open symbols stand for experimental data; solid line is calculated result using Eq.(3).

peak at T_p may be attributed to the phase competition of AFM and PM phases for $\text{Nd}_{0.5}\text{Ca}_{0.5}\text{MnO}_3$. These results give a direct evidence of spin-phonon coupling in the compound. With Al doping, the ultrasonic attenuation peak at T_p shifts to lower temperature. We suggest that this ultrasonic effect is the result of the partial suppression of CE-type AFM in $\text{Nd}_{0.5}\text{Ca}_{0.5}\text{MnO}_3$ due to the Al doping.

IV. CONCLUSION

The ultrasonic, magnetic and transport properties of $\text{Nd}_{0.5}\text{Ca}_{0.5}\text{Mn}_{1-x}\text{Al}_x\text{O}_3$ ($x=0,0.03$) have been studied. The ultrasonic anomaly around the charge ordering transition temperature T_{CO} gives direct evidence for electron-phonon coupling in the compound. At low temperature, a slight softening in sound velocity and a large attenuation peak were observed. The results provide a trace of separation between the AFM and PM phases and give direct evidence for spin-phonon coupling in the compound. The study shows that Al doping partially suppresses the charge ordering and CE-type AFM state in $\text{Nd}_{0.5}\text{Ca}_{0.5}\text{MnO}_3$.

V. ACKNOWLEDGMENTS

This work was supported by the National Natural Science Foundation of China (No.10274075) and the Specialized Research Fund for the Doctoral Program of Higher Education (No.20030358056).

- [1] S. Jin, T. H. Tiefel, M. McCormack, R. A. Fastnacht, R. Ramesh and L.H. Chen, *Science* **264**, 413 (1994).

- [2] R. Von Helmolt, J. Wecker, B. Holzapfel, L. Schultz and K. Samwer, *Phys. Rev. Lett.* **71**, 2331 (1993).
- [3] K. Chahara, T. Ohno, M. Kasai and Y. Kozono, *Appl. Phys. Lett.* **63**, 1990 (1993).
- [4] N. Liu, G. Q. Yan and W. Tong, *Chin. J. Chem. Phys.* **18**, 589 (2005).
- [5] S. Mori, C. H. Chen and S. W. Cheong, *Nature (London)* **392**, 473 (1998).
- [6] S. Mori, C. H. Chen and S. W. Cheong, *Phys. Rev. Lett.* **81**, 3972 (1998).
- [7] N. R. Rao and A. K. Cheetham, *Science* **276**, 91 (1999).
- [8] Y. Tokura and N. Nagaosa, *Science* **288**, 462 (2000).
- [9] H. Kuwahara, Y. Tomioka, A. Asamitsu, Y. Moritomo and Y. Tokura, *Science* **270**, 961 (1995).
- [10] Y. Tomioka, A. Asamitsu, Y. Moritomo, H. Kuwahara and Y. Tokura, *Phys. Rev. Lett.* **74**, 5108 (1997).
- [11] H. Y. Huang, S. W. Cheong, P. G. Radaelli, M. Marezio and B. Batlogg, *Phys. Rev. Lett.* **75**, 914 (1995).
- [12] A. Urushibara, Y. Moritomo, T. Arima, A. Asamitsu, G. Kido and Y. Tokura, *Phys. Rev. B* **51**, 14103 (1995).
- [13] V. Hardy, A. Maignan, S. Hebert and C. Martin, *Phys. Rev. B* **67**, 24401 (2003).
- [14] G. Allodi, R. De Renzi, F. Licci and M. W. Pieper, *Phys. Rev. Lett.* **81**, 4736 (1998).
- [15] A. J. Millis, P. B. Littlewood and B. I. Shraiman, *Phys. Rev. Lett.* **74**, 5144 (1995).
- [16] A. J. Millis, B. I. Shraiman and R. Mueller, *Phys. Rev. Lett.* **77**, 175 (1996).
- [17] F. Millange, S. de Brion and G. Chouteau, *Phys. Rev. B* **62**, 5619 (2000).
- [18] T. Vogt, A. K. Cheetham, R. Mahendiran, A. K. Raychaudhuri, R. Mahesh and C. N. R. Rao, *Phys. Rev. B* **54**, 15303 (1996).
- [19] F. Dupont, F. Millange, S. de Brion, A. Janossy and G. Chouteau, *Phys. Rev. B* **64**, 220403 (2001).
- [20] R. W. Li, J. R. Sun, Q. A. Li, Z. G. Wang, S. Y. Zhang, Z. H. Cheng, H. W. Zhao and B. G. Shen, *J. Appl. Phys.* **91**, 7941 (2002).
- [21] A. P. Ramirez, P. Schiffer, S. W. Cheong, C. H. Chen, W. Bao, T. T. M. Palstra, P. L. Gammel, D. J. Bishop and B. Zagarshi, *Phys. Rev. Lett.* **76**, 3188 (1996).
- [22] C. F. Zhu, R. K. Zheng, J. R. Su and J. He, *Appl. Phys. Lett.* **74**, 3504 (1999).
- [23] C. F. Zhu and R. K. Zheng, *J. Phys: Condens. Matter.* **11**, 8505 (1999).
- [24] R. K. Zheng, C. F. Zhu, J. Q. Xie and X. G. Li, *Phys. Rev. B* **63**, 024427 (2001).
- [25] H. Kong and C. F. Zhu, *Appl. Phys. Lett.* **88**, 041920 (2006).
- [26] H. Kong, J. Q. Xie, S. L. Zhang, J. R. Su and C. F. Zhu, *Acta. Meta. Sini.* **39**, 1183 (2003).
- [27] N. F. Mott and E. A. Davies, *Electronic Processes in Noncrystalline Solid*, 2nd edn., Oxford: Clarendon Press, 1 (1979).
- [28] M. Cankutaran, G. A. Saunders, K. C. Goretta and R. B. Poeppel, *Phys. Rev. B* **46**, 1157 (1992).
- [29] R. L. Melcher, *Physical Acoustics*, New York: Academic, 1 (1976).
- [30] H. Hazama, T. Goto, Y. Nemoto, Y. Tomioka, A. Asamitsu and Y. Tokura, *Phys. Rev. B* **62**, 15012 (2000).
- [31] K. I. Kugel and D. I. Khomskii, *Usp. Fiz. Nauk* **136**, 621 (1982); *Sov. Phys. Usp.* **25**, 231 (1982).